

The LLCL filter-based synchronverter with adaptive fuzzy logic controller

Tan Thien Tran^{1,2,3}, Quoc Dung Phan^{1,2}, Bao Anh Nguyen^{1,2}, Weng Kean Yew⁴

¹Faculty of Electrical and Electronics Engineering, Ho Chi Minh City University of Technology (HCMUT), Ho Chi Minh City, Vietnam

²Vietnam National University Ho Chi Minh City (VNU-HCM), Ho Chi Minh City, Vietnam

³System Operator Department, Southern Regional National Load Dispatch Centre, Ho Chi Minh City, Vietnam

⁴School of Engineering and Physical Sciences, Heriot-Watt University Malaysia, Putrajaya, Malaysia

Article Info

Article history:

Received Feb 18, 2024

Revised Jul 6, 2024

Accepted Jul 24, 2024

Keywords:

Fuzzy logic controller
LLCL filter
Renewable energy sources
Synchronverter
Virtual inertia
Virtual synchronous generator

ABSTRACT

Global warming has emerged as a significant issue, primarily due to the use of fossil fuels for power generation. Renewable energy adoption has surged. However, stability issues arise when integrating the primary source and inertia-less nature of converter-interfaced renewable energy sources (RESs) into the traditional power system, due to its intermittent and uncertain nature. The proposed solution involves controlling converter-interfaced RES to emulate the characteristics of a conventional synchronous generator (SG), commonly known as a virtual synchronous generator or synchronverter. As it fundamentally functions as a power converter, it is crucial to consider the appropriate filter design for the synchronverter. Additionally, by emulating the characteristics of SG, the values of “virtual” inertia and droop coefficients must be chosen accurately to provide a robust response under different operating scenarios of the synchronverter. Hence, this paper proposes a novel LLCL filter-based synchronverter system along with an adaptive control strategy using a fuzzy logic controller (FLC). The system is simulated under different operating scenarios in MATLAB/Simulink. The proposed system demonstrated improved frequency response and reduced total harmonic distortion compared to the conventional synchronverter model for all the different operating scenarios, thus enhancing grid stability and power quality.

This is an open access article under the [CC BY-SA](https://creativecommons.org/licenses/by-sa/4.0/) license.



Corresponding Author:

Quoc Dung Phan

Faculty of Electrical and Electronics Engineering, Ho Chi Minh City University of Technology (HCMUT)

Vietnam National University Ho Chi Minh City (VNU-HCM)

268 Ly Thuong Kiet Street, District 10, 72506, Vietnam

Email: pqdung@hcmut.edu.vn

1. INTRODUCTION

Transitioning to renewable energy is an effective way of reducing the carbon footprint in electrical generation. However, stability issues arise when integrating primary source and inertia-less nature of converter-interfaced renewable energy sources (RESs) into the traditional power system, due to its intermittent and uncertain nature. Thus, this has posed a significant challenge for the power grid. When faced with an extreme condition of low inertia and insufficient power reserve, load shedding has to be activated in order to prevent loss of synchronism or blackouts [1], [2]. As a result, significant efforts have been devoted to studying and implementing control strategies for converter-interfaced RES to support the grid under normal and extreme conditions. One of the emerging fields is the grid-forming control strategy, notably the virtual synchronous generator, also known as the synchronverter model, offers a promising solution for controlling converter-interfaced RESs by emulating the characteristics of synchronous generator (SG) in the power grid [2]–[7].

There have been different studies conducted under the general term “virtual synchronous generator/machine”. The first approach, proposed in a study by Beck and Hesse [8] and called virtual synchronous machine (VISMA), derives the seventh-order model of the synchronous generator (SG) into the control system. This approach inherits all the characteristics of the SG but exhibits poor dynamics behavior under islanding operation and complexity in implementation [4]. In contrast, many studies have been conducted under the names synchronverter and virtual synchronous generator (VSG) using low-order equations of the SG due to their simplicity and good performance. The VSG is based on the application of the SG swing equation in the control strategy [2]–[4], [6], [7], [9], [10]. The synchronverter model, on the other hand, describes the mathematical equations of the stator and rotor of the SG. Moreover, the application of the synchronverter model for converter interfaced RESs is easier when compared with the VSG model since the performance of the VSG depends on many parameters and components of controller. Therefore, the synchronverter model will be further studied and applied in this paper.

The concept “synchronverter” allows converter interfaced RESs to mimic the principles of SG and has been well-developed further in previous studies [11], [12]. Research on the synchronverter model varies across various aspects. Preview study by Zhong and Weiss [13], an introduction to the synchronverter-based control strategy for power systems and microgrid applications is proposed. Additionally, research on improving the dynamic response under fault conditions of the synchronverter is presented in study by Schulze *et al.* [14]. Control parameter design and tuning methods for the synchronverter are proposed in Dong and Chen [15] based on mathematical analysis. Moreover, Rodríguez-Cabero *et al.* [16] extensively present the relationship of parameters in the stability performance of the entire system using small signal analysis. This helps in determining parameters for the synchronverter for stable operation. Parallel operation of multi-synchronverter systems is also a trending research topic. Yap *et al.* [17] propose adaptive control strategies using fuzzy control system. Lastly, the study of filter design and its contribution to the stable operation of the synchronverter has been examined, albeit only with the LCL filter [18]–[20]. In the aspect of adaptive control, research has been conducted on adaptive damping, control, or self-adaptive synchronverters, as mentioned in previous studies [17], [21], [22]. However, Wang *et al.* [22] only focus on the switching method with fixed values of control parameters. On the other hand, Li *et al.* [21] provide online calculation of both droop and inertia values but following a fixed control rule. In contrast, Yap *et al.* [17] employ fuzzy logic control (FLC) along with optimization methods to calculate more adaptive control parameters, but it is a time-consuming task. The applications of FLC for determining “adaptive” control values of both inertia and droop coefficients to which follow different operating scenarios in synchronverter systems have not been explored yet. Furthermore, the utilization of the LLCL filter, which offers better performance in harmonic limitation compared to the LCL filter, has not been studied or implemented in synchronverter systems.

Therefore, this paper proposes a novel LLCL filter based synchronverter system, along with an FLC-based adaptive control system to determine both inertia and droop coefficient values under different operating conditions. The paper is divided into four parts: i) Studies on VSG and Synchronverter system together with research gap are introduced in Section 1, ii) Section 2 provides the background of the system and the proposed adaptive control strategy based on FLC, iii) Section 3 outlines the case studies and the respective simulation results, and iv) Section 4 summarizes the findings of the proposed system.

2. MATHEMATICAL MODEL OF THE LLCL FILTER-BASED SYNCHRONVERTER SYSTEM

The following subsections provide a brief description of the theoretical background of the conventional synchronverter model. Firstly, a mathematical model of the conventional synchronverter is presented. Then, the well-known LLCL filter is shown with a brief comparison to the LCL filter. Finally, the control method deriving fuzzy for the proposed control strategy of the LLCL filter-based synchronverter system is provided.

2.1. Synchronverter model

The first model of synchronverter, described in study [13], derived the swing equation of a synchronous generator as the active power loop (APL) to control the virtual rotor angle and active power output. Additionally, the reactive power loop (RPL) was implemented to adjust the reactive power generation and voltage magnitude at the terminal of the synchronverter. The mathematical equation describes the RPL is expressed as (1).

$$K_g \frac{d\psi_f}{dt} = (Q_g^* - Q_{tf}) + S_q \sqrt{\frac{2}{3}} D_q (U_t^* - U_{tf}) \quad (1)$$

Where Q_g and U_t are reactive power generation and terminal voltage of synchronverter, respectively; the upper script “*” stands for the setting/reference value. ψ_{ff} is the virtual field flux. The reactive droop

coefficients D_q and RPL response speed parameter K_g can be chosen as in research [23]. The under script “f” defines the filtered signals through the low-pass filter with the time constant T_f also defined in research [23]. Then, Dong and Chen [24] proposed an active damping correction loop to enhance the dynamic response speed of the APL. The general mathematical equations describing the synchronverter are provided in researches [15], [23]–[25], and expressed as in (2).

$$J_g \frac{d\psi_f}{dt} = T_m - T_{ef} + D_p(\omega_g^* - \omega_g) - D_f \frac{d}{dt} \left(\frac{T_{ef}}{\psi_{ff}} \right) \quad (2)$$

Where J_g is virtual inertia coefficient, T_m and T_{ef} are mechanical and electrical torque of synchronverter, D_p and D_f are droop and damping parameters of the APL and active damping loop, respectively, ω_g and ω_g^* are the output and reference angular velocity of the synchronverter. Output voltages of the synchronverter are then described by (3). Furthermore, the self-synchronism property of SG is emulated by employing the control strategy outlined in study [23]. These control phases fulfill the capability of emulating the characteristics of SG in the synchronverter. In this paper, the conventional model described in study [15] and applied with certain modifications for the LLCL-based synchronverter system.

$$e = \theta \psi_f [\sin(\theta) \quad \sin(\theta + 2\pi/3) \quad \sin(\theta - 2\pi/3)] \quad (3)$$

2.2. LLCL filter

The recent passive LLCL filter, with an additional inductor in the capacitor trap circuit, have made it superior to the traditional LCL, especially in switching harmonics limitation [26]. With output transfer functions, the responses of the LLCL- and LCL-based converter system do not show many differences in the low frequency range. Then, the LLCL-based synchronverter system will be deployed for the first time to analyze performances of the proposed adaptive control strategy using FLC. Huang *et al.* [26] also proposed details about the LLCL filter design procedure and constraints which will be applied as design guidelines in this paper.

2.3. Adaptive control strategy with fuzzy logic controller

This paper proposes an adaptive FLC-based control strategy for the synchronverter system with an LLCL filter. The fuzzy logic controller consists of three main parts [27]. The fuzzification phase aids in transforming crisp sets of input values into fuzzy membership functions. The second part is the fuzzy inference engine, which includes the rule base where the relationships between inputs and outputs states are defined. Finally, the defuzzification process translates the fuzzy output values into the crisp values.

3. THE PROPOSED METHOD OF CONTROL STRATEGY FOR THE LLCL FILTER BASED SYNCHRONVERTER SYSTEM

The design procedure and simulation of the proposed method of control strategy for the LLCL filter based synchronverter system are inherent in previous researches [15], [25]. Since the synchronverter model itself is based on the study by Dong and Chen [15] and with the purpose of comparison to previous studies in order to clarify the advantages of the proposed system. Table 1 presents the parameters utilized for filter design and simulation. These parameters are referenced from [15], [25] for the purpose of comparison.

Table 1. System parameters

Notation	Parameters	Values	Notation	Parameters	Values
Sb	Rated/base power	1.6 MVA	VDC	DC link voltage	13 kV
Vb	Rated/base line-line voltage	6.6 kV	Df	Active damping coefficient	1.13 Vs ² /rad
fb	Rated/base frequency	60 Hz	Dq	RPL droop coefficient	3711 var/V
ωb	Rated/base angular frequency	377 rad/s	Kg	Integrator parameter in the RPL	27980 var.rad/V
fsw	Switching frequency	12 kHz	Tf	Low-pass filter time constant	0.01 s
Ts	Sampling time	833.33 ns			

3.1. LLCL filter parameters

Following the design constraints and procedure outlined in study by Huang *et al.* [26], the parameters of the LLCL filter employed in this paper are then determined. In addition, the design process for the LCL filter is similar to that of the LLCL filter. The parameters for the LLCL and LCL filters are presented in Table 2 along with some comments as follows. Firstly, the grid-side inductance of the LLCL filter is significantly reduced compared to the LCL filter which then helps in lowering total mass and capital requirements for the LLCL filter while still maintaining the ability to limit harmonics. Then, the damping resistance in the trap

circuit of the LLCL filter is much smaller, which helps to reduce the power loss of the filter. Finally, with the additional inductance in the trap circuit, the LLCL filter exhibits better performance in limiting harmonics around the switching frequency. Figure 1 illustrates the Bode plot of the transfer functions for the LCL filter (dashed blue line) and LLCL filter (solid red line) with the design parameters presented in Table 2.

Table 2. Filter design parameters

Parameters	LLCL filter	LCL filter
Converter side inductance (L_1 , [mH])	3.6	3.6
Grid side inductance (L_2 in [mH])	0.32	0.64
Capacitance of resonance branch (C_f , [μ F])	2.14	2.14
Damping resistance (R_d , [$m\Omega$])	0.3	8.3
Inductance of resonance branch (L_f , [μ H])	82	-

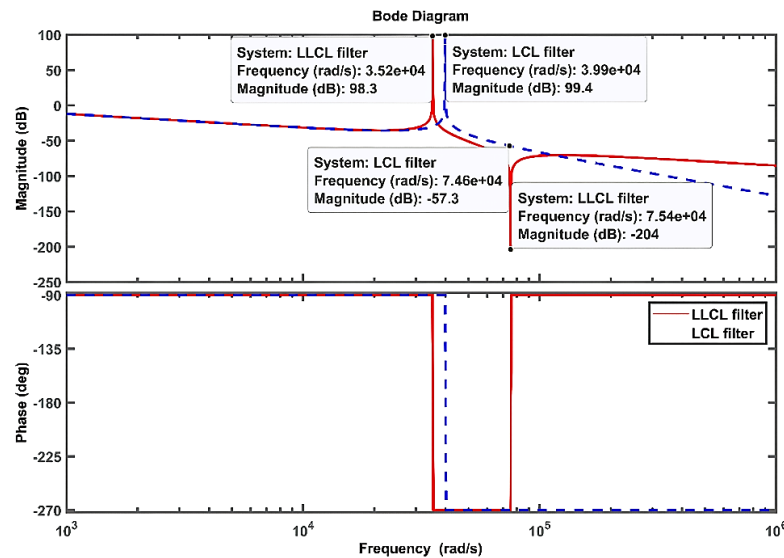


Figure 1. Bode plot of the designed LLCL and LCL filter

3.2. The adaptive control strategy based on fuzzy logic controller

The FLC system in the proposed control strategy are illustrated in Figure 2. The normalized frequency deviation and the rate of change of frequency deviation are utilized as inputs for the fuzzy system while the outputs correspond to the values of the virtual inertia (J_g) and active power droop (D_p) coefficients. To ensure consistency, the input variables are normalized within the range of $[-1, 1]$. Additionally, the rate of change of frequency deviation input is sampled at a time frame of approximately 83.3 ms to mitigate sub-transient noises while still capturing the evolution of the system's frequency variation [28]. Drawing upon the principles outlined in [21], the attributes and numbers of membership functions together with the rule base can be varied based on system design expert. Then, leveraging accumulated experience from simulation practices, the proposed FLC-based control strategy in this paper adopts trapezoidal membership functions together with the rule base as; the five input attributes are classified as: negative big (NB), negative small (NS), zero (Z), positive small (PS), and positive big (PB). Similarly, the outputs employ type II Gaussian membership functions and are defined as: low (l), medium (m), and high (h), as shown in Figure 2(a) and Figure 2(b). The 5x5 rule base table for the fuzzy inference engine which visually represents the membership functions of the inputs, outputs, and the rule base of the fuzzy inference engine utilized in the proposed control strategy, respectively, is given in Figure 2(c).

3.3. The LLCL filter-based synchronverter system with the proposed adaptive control strategy

Figure 3 until Figure 5 depict the simulation models implemented in the MATLAB/Simulink environment for the LLCL based synchronverter system with the proposed control strategy. These simulation models include the control block diagram and represent the integration of the FLC and LLCL filter into the synchronverter system. Figure 3 shows the control block diagrams of the APL with active damping as in (2) and RPL as in (1) [23]-[25] where the adaptive coefficients of virtual inertia (“ J_g _fuzzy”) and droop (“ D_p _fuzzy”) are calculated by the FLC. As observed from the control model, changes in the values of the virtual inertia and droop coefficients directly affect the virtual rotor angle (“theta”), thereby adjusting the

frequency response of the synchronverter. Then from the voltage magnitude with virtual rotor angle as in (3), reference voltage control signals for the synchronverter are created [15], as shown in Figure 4. Lastly, Figure 5 showcases the complete LLCL based synchronverter system with the proposed control strategy outlined in this paper. A two-level three-phase inverter that functions as the synchronverter and encapsulates the integration of the LLCL filter, FLC, and the synchronverter system.

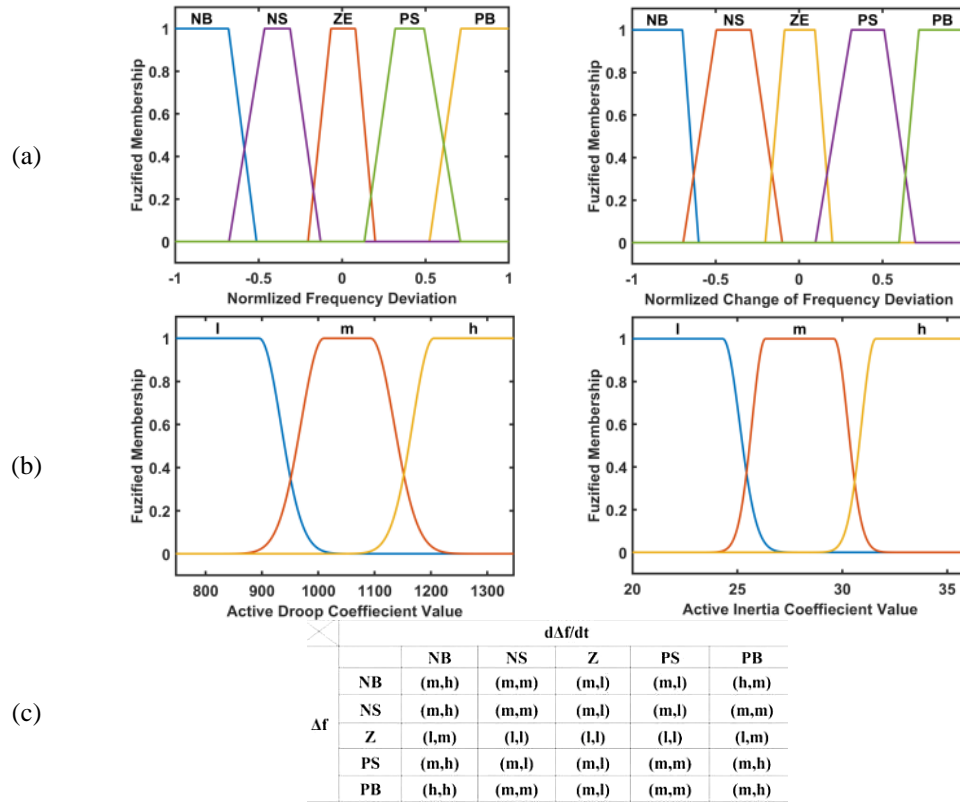


Figure 2. The proposed FLC with membership functions of (a) inputs, (b) outputs, and (c) rule base for the proposed fuzzy inference engine

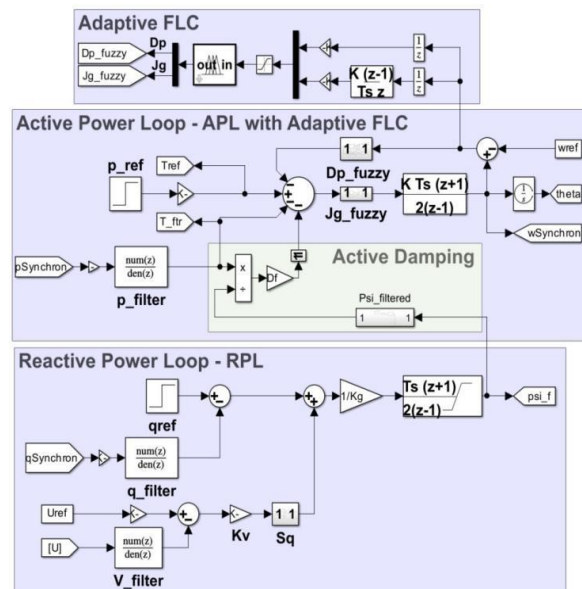


Figure 3. Control block diagram of the proposed system

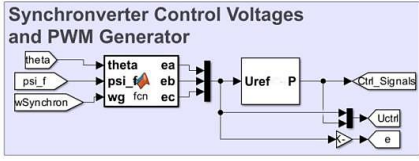


Figure 4. Control signals block diagram for the proposed LLCL based synchronverter system

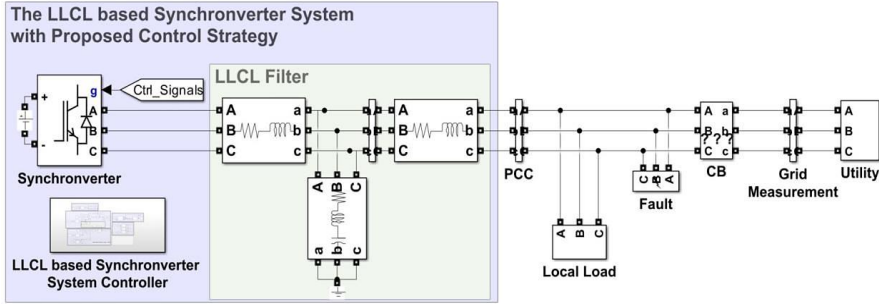


Figure 5. General simulation model of the proposed system

Based on the provided model figures, the proposed system differs from the conventional model in the following. Firstly, the online values of virtual inertia and droop coefficients are obtained from the proposed adaptive FLC-based control strategy. Then, the LLCL filter-based synchronverter system in this paper omits a proportional integral (PI) controller in the APL, which is otherwise required for the self-synchronization capability of the conventional model [24], [27]. This introduces the novel implementation of the LLCL filter in the synchronverter system.

4. SIMULATION RESULTS & DISCUSSION

In this section, simulation results of the LLCL filter based synchronverter system with the proposed control strategy are presented under various operating scenarios. The frequency response of the synchronverter system in this paper is compared to the conventional model described in studies [15], [25], highlighting the advantages in terms of islanding and grid-connected operation. Additionally, the LLCL filter's capability to limit harmonics is evaluated by comparing it with the LCL filter based synchronverter model.

4.1. Case studies

Figure 5 shows the general simulation model in MATLAB/Simulink which parameters are given in Table 1 and Table 2. The simulation includes three main cases that represent different operating conditions to highlight the capabilities of the proposed LLCL filter based synchronverter system and compare it to conventional models from previous studies. The details of these cases are:

- **Islanding mode:** This case simulates the system operating in islanded mode, where the synchronverter is disconnected from the grid and supplies power to local loads. The islanding mode simulation runs from 0.8 to 3.2 s and includes the following events: At 1.8s, a three-phase fault scenario occurs and lasts for 200 ms, representing a fault in the local distribution system. At 2.4 s and 2.8 s, there are increases in the local load by 30% of the rated power, representing changes in the load demand. Then, at 3.2s, the system transitions back to grid-tied operation.
- **Grid-tied operation:** This case represents the synchronverter being connected to the grid and operating in synchronization with the grid. The simulation runs from 3.2 to 5 s and includes the following events: At 3.6 s, there is an increase in the reference active power generation, representing a change in the desired power output of the synchronverter. Then, from 4 to 4.5 s, a grid frequency contingency of decreasing 1% rated value occurs, representing a disturbance in the grid frequency.
- **Comparisons between the proposed system with the conventional model under control strategy perspective:** In this case, the system performances of currents and voltages are then evaluated between proposed control strategy of the LLCL-based synchronverter system with the conventional model in studies [23]–[25] and includes the following events: At 1s the system is in island mode operation then at 2 s, the system is reconnected to utility.

These simulation cases are designed to assess the performance of the proposed LLCL filter based synchronverter system and its control strategy under different operating conditions, including fault scenarios, load changes, and grid disturbances. By comparing the results to conventional models, the advantages, and improvements of the proposed system can be evaluated.

4.2. Simulation results & discussion

4.2.1. Under islanding mode operation

In Figures 6(a) and 6(b), the frequency response and active power generation of the synchronverter models under islanding operation (from 0.8 to 3.2 s) are shown, while Figure 6(c) displays the values of inertia and droop coefficients obtained via the FLC in the proposed control strategy of the LLCL filter-based synchronverter system. Figure 6(b) demonstrates that the proposed system successfully provides inertia response, self-synchronism, and governor response, enabling stable islanding operation with continuous power generation. The response of the proposed system, equipped with either the LLCL or LCL filter, shows similarity to conventional models.

This suggests that the type of filter does not significantly impact the active power generation response of the synchronverter, assuming that active power losses in the filter are negligible. In contrast, Figure 6(a) reveals significant differences in the frequency response between the proposed system and the conventional synchronverter model. The proposed system reaches a steady state approximately 0.25 s after the islanding state with a small amplitude and highly damped oscillation, represented by the black line in Figure 6(a). In contrast, the conventional model takes nearly three times longer to reach a steady state and exhibits substantial high-amplitude oscillation, represented by the red and blue dashed lines in Figure 6(a). The amplitude of the oscillations in the conventional model is approximately 5% of the rated value and decays slowly after 0.75 s.

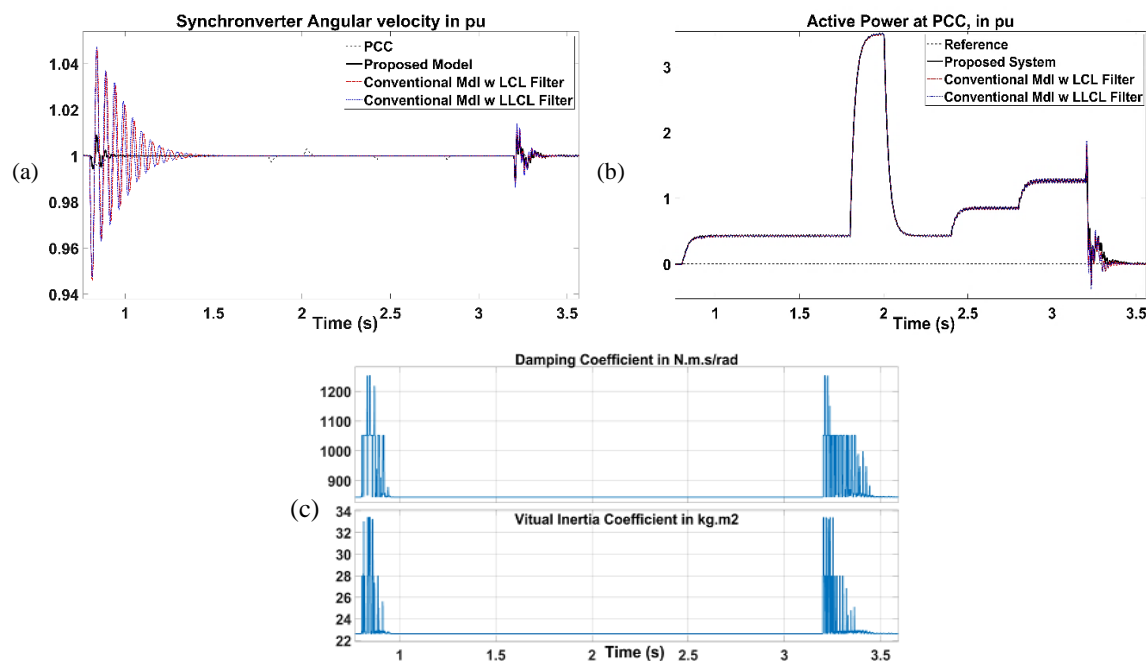


Figure 6. Responses of synchronverter models: (a) frequency, (b) active power generation of synchronverter models at the point of common coupling (PCC), and (c) output values of droop and inertia parameters using FLC in the LLCL filter based synchronverter system with the proposed control strategy

This notable difference in performance can be attributed to the proposed control strategy, particularly the adaptive determination of inertia and droop coefficients under different scenarios, as shown in Figure 6(c). The proposed system outperforms the conventional model, which employs a virtual impedance obtained through trial-and-error and an additional PI controller in the active power loop (APL) to achieve self-synchronization capability. The proposed system, in contrast, omits the PI controller and employs randomly fixed values for the virtual impedance, yet still provides a better frequency response as mentioned before.

Figures 7(a)-7(d) display the total harmonic distortion of the current (THD_i) values for the LLCL, LCL filter-based synchronverter models under a 3-phase fault are shown in Figures 7(a)-7(b) and high load demand are shown in Figures 7(c)-7(d). Figures 7(e)-7(f) present the total harmonic distortion of the voltage (THD_v)

values for the LLCL and LCL filter-based synchronverter models under high load demand. From Figures 7(a)-7(d), it can be observed that the THD_i values of the LLCL filter-based synchronverter are approximately half of those of the LCL-based model. The same trend is observed for the THD_v values in Figures 7(e)-7(f) under islanding operation. This demonstrates the superior harmonic limitation capabilities of the LLCL filter compared to the LCL filter. Furthermore, as shown in Figures 7(a)-7(f), the magnitudes of harmonics around the switching frequency of the LCL filter-based synchronverter model are over twenty times that of the LLCL under different scenarios. These results provide strong evidence of the superior harmonic limitation capabilities of the LLCL filter over the LCL filter, particularly under the islanding operation of the synchronverter model.

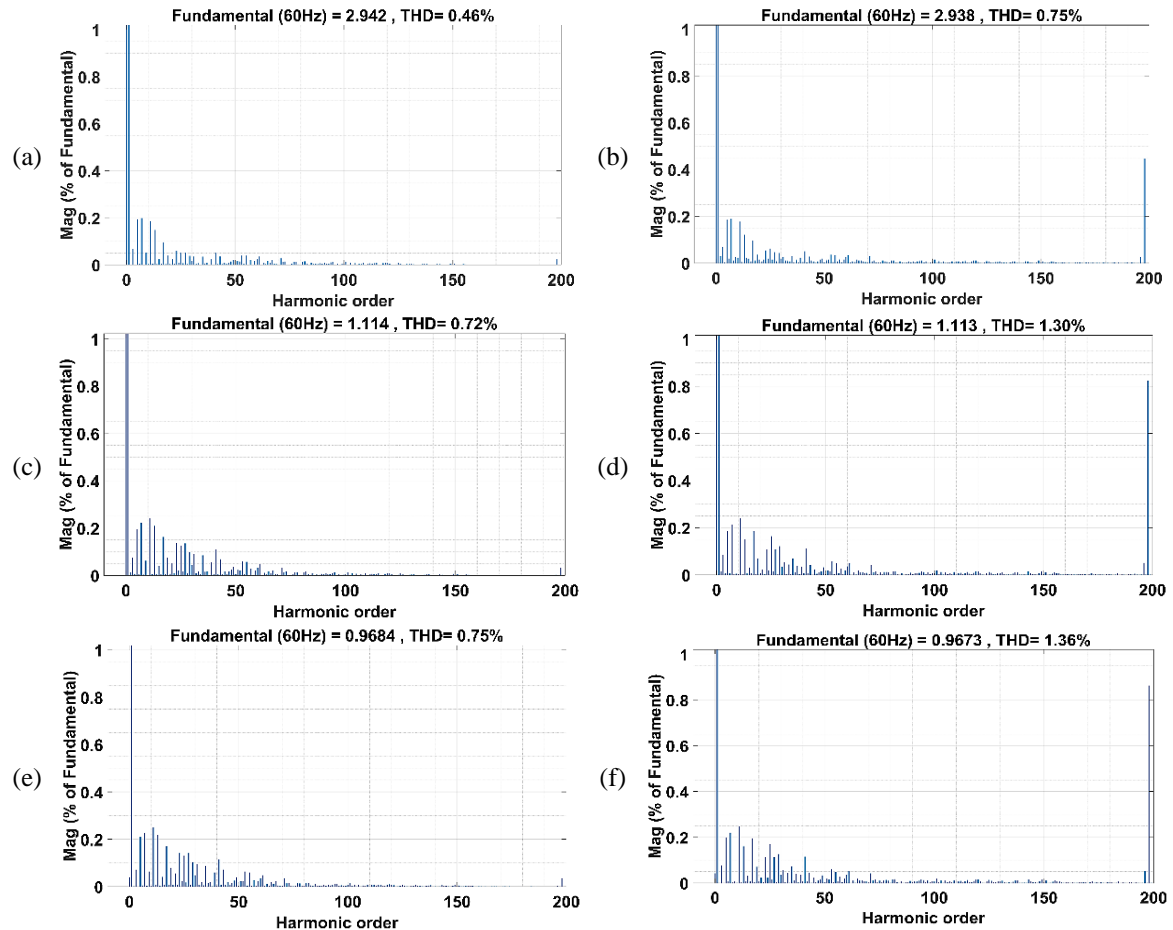


Figure 7. THD values of output currents and voltage of proposed model under islanding operation-based synchronverter model: (a) THD_i under 3P fault scenario of LLCL filter, (b) THD_i under 3P fault scenario of LCL filter, (c) THD_i under high load scenario of LLCL filter, (d) THD_i under high load scenario of LCL filter, (e) THD_v under high load scenario of LLCL filter, and (f) THD_v under high load scenario of LCL filter

4.2.2. Under the grid-tied operation

The scenarios under grid-tied operation are designed to examine the power generation capabilities under normal conditions and grid support capabilities during contingencies of the proposed system. Figures 8(a) and 8(b) show the frequency and active power responses of the proposed system and conventional models under different operating scenarios. As shown in Figure 8(b), the active power generation of all models follows the reference value within 0.4 s and without any overshoot. Due to the rule base applied in the fuzzy inference engine of the proposed system, there are slight changes in the values of inertia and droop parameters, resulting in similar frequency and active power responses between the models under a frequency contingency period, as depicted in Figures 8(b) and 8(c). Furthermore, in Figure 8(a), the synchronverter demonstrates its capability to emulate inertia response of a synchronous generator (SG), particularly in supporting the grid during contingencies. Figures 9(a)-9(d) present THD_i values of LLCL and LCL filter-based synchronverter models under changes in the reference active power (Figures 9(a) and 9(b)) and grid frequency contingency

(Figures 9(c) and 9(d)). Similarly, from Figures 9(a)-9(d), the THD_i values of LLCL filter-based synchronverter are lower than those of the LCL-based model. In addition, the magnitudes of harmonics around switching frequency of the LLCL-based synchronverter system are significantly lower than that of the LCL based, the same as operating under islanding mode in Figure 7. Therefore, these results further emphasize the superior harmonic limitation capabilities of the LLCL filter-based synchronverter system over the LCL filter under both islanding and grid-tied operations across different scenarios.

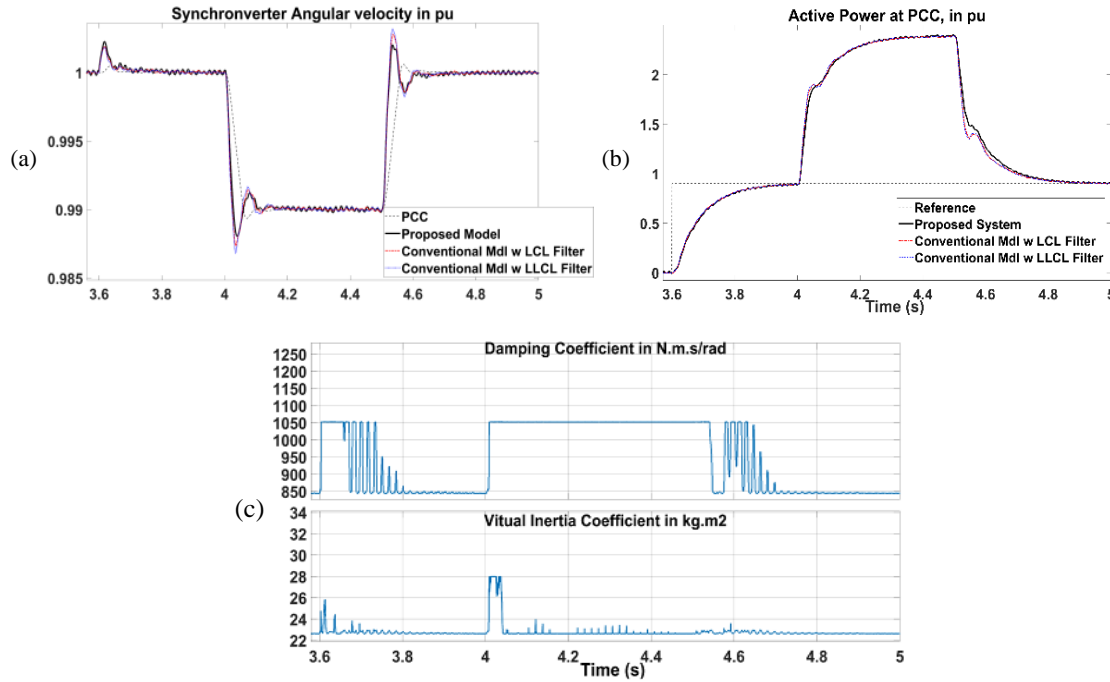


Figure 8. Responses of (a) frequency response of synchronverter models, (b) active power generation of synchronverter models at PCC, and (c) output values of droop and inertia parameters using FLC in the LLCL filter based synchronverter system with the proposed control strategy

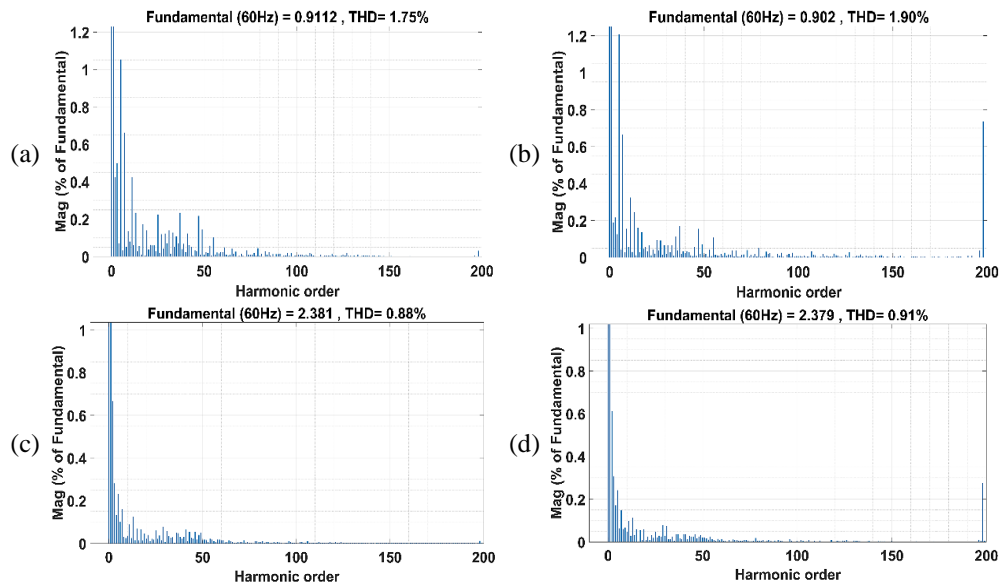


Figure 9. THD values of output currents and voltage of proposed model under grid-tied operation: (a) THD_i under changes in the reference active power of LLCL filter based synchronverter model, (b) THD_i under changes in the reference active power of LCL filter based synchronverter model, (c) THD_i under grid frequency contingency of LLCL filter based synchronverter model, and (d) THD_i under grid frequency contingency of LCL filter based synchronverter model

4.2.3. Comparison between the proposed control strategy and conventional synchronverter systems

The conventional model in [23]-[25] requires a virtual impedance together with a PI controller to obtain the self-synchronism characteristic of the synchronous generator. Parameters of the virtual impedance and PI controller need choosing carefully in order to obtain smooth dynamic response. Table 3 shows the sub-study cases with different sets of control parameters of the conventional model that have been conducted in simulation to evaluate performances to the proposed system. Figures 10(a)-10(b) show simulation results of output current at PCC and frequency response between the proposed system and conventional model with sub-study cases under island mode operation.

Then, Figures 10(c) and 10(d) show simulation results of output current at PCC and frequency response between the proposed system and conventional model with sub-study cases under grid-tied operation. From the simulation results, some comments are derived as follows. Firstly, the transient responses between the proposed system and conventional model with sub-study cases show similarity in output current dynamics under grid-connected contingency, as shown in Figures 10(a), 10(c), and 10(d). However, the conventional model of sub-study case No.4 shows poor dynamic performance as in Figure 10(c). However, a major improvement of frequency response under islanding contingency is obtained via the proposed system with a fast response to steady state and low overshoot, as shown in Figure 10(b) with the black line.

Table 3. Control parameters of the proposed system and conventional model with sub-study cases

Model	Virtual impedance	PI controller parameters	Virtual damping (droop) and inertia coefficient
The LLCL based synchronverter system with proposed control strategy	Fixed ($L_v = 2 \text{ mH}$, $R_v = 0.0369 \Omega$)	Eliminated	Adaptive based on FLC
Conventional model Case 1	$L_v = 2.1 \text{ mH}$, $R_v = 0.0464 \Omega$	$K_p = 5$; $k_i = 50$;	Fixed
Case 2	$L_v = 0.848 \text{ mH}$, $R_v = 0.0224 \Omega$	$K_p = 40$; $k_i = 10$;	Fixed
Case 3	$L_v = 2.1 \text{ mH}$, $R_v = 0.0679 \Omega$	$K_p = 2$; $k_i = 80$;	Fixed
Case 4	$L_v = 1.4 \text{ mH}$, $R_v = 0.0224 \Omega$	$K_p = 40$; $k_i = 10$;	Fixed

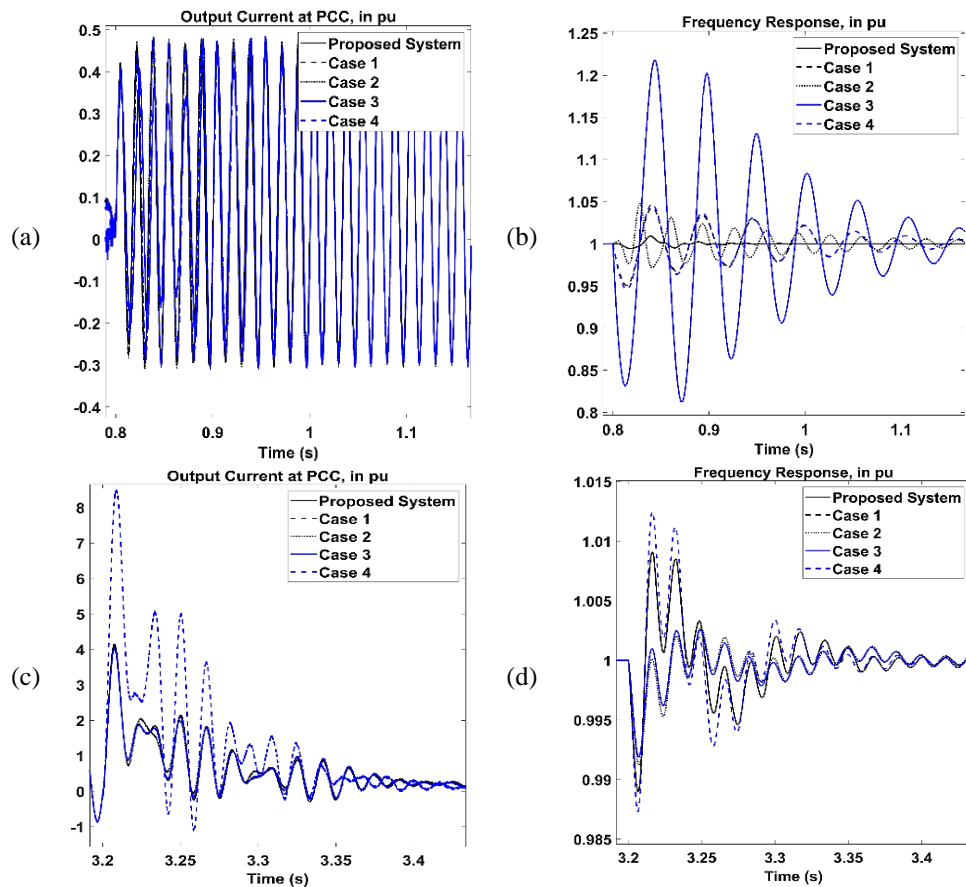


Figure 10. Transient responses between the proposed system and conventional model under different sub-study cases with: (a) output current, (b) frequency variation of the synchronverter system under disconnecting to utility, (c) output current, and (d) frequency variation of the synchronverter system under grid tied operation

Secondly, from Figure 10(b), the conventional model cases show low damping oscillations with high amplitude, the amplitude of oscillation can be improved by choosing appropriate coefficients of the PI controller, but a slow steady state still remains. Furthermore, in the conventional model, the parameters of the controller and virtual impedance must be determined in order to obtain a fine response. Furthermore, the interval between grid-connected and island mode of the conventional model cannot be too small since it requires more time to get to a steady state [23], in simulation results shown in Figure 10 it requires more than 0.5 s. In contrast, the proposed system with FLC has eliminated the PI controller, and virtual impedance parameters are easily determined and fixed, as shown in the above simulation results. Table 4 shows comparisons between the LLCL-based synchronverter system with FLC-based adaptive control strategy and the studied control strategy of synchronverter models on the control values, input parameters, and complexity of the control strategy. The proposed system in this paper obtains smooth output performances as analyzed above with low order of complexity.

Table 4. Comparisons of the studied synchronverter models and the LLCL-based synchronverter system with adaptive FLC

Scheme	Control values	Parameters considered for control strategy	Complexity
Adaptive control using fixed rules [15], [16]	Droop and inertia parameters	FrDe and RoCoF	Low - fixed values of control parameters leading oscillation
Fuzzy logic application with GA method [22]	Virtual inertia	FrDe, RoCoF, and penetration Level of non-SG	High - approaching only one control parameter
The proposed LLCL based synchronverter system	Droop and inertia parameters	FrDe and RoCoFrDe	Low - approaching both control parameters with continuous values

5. CONCLUSIONS

This study introduces a control strategy utilizing a fuzzy logic controller to determine adaptive values for virtual inertia and droop coefficients. The primary aim is to enhance the frequency responses of LLCL filter-based synchronverter systems during both grid-tied and islanding operations. The LLCL filter is implemented for the first time in the synchronverter model to mitigate harmonics, particularly those arising around the switching frequency.

Simulation results demonstrate that the proposed adaptive control strategy for LLCL filter-based synchronverter systems significantly improves frequency response during islanding and grid-connected transient conditions compared to conventional synchronverter models. Furthermore, the proposed system eliminates the need for a meticulously designed virtual impedance and a PI controller, which are typically prerequisites for the self-synchronization functionality in conventional synchronverter models. Across various simulation scenarios, the proposed model incorporating the LLCL filter exhibits reduced total harmonic distortion in both output current and voltage, notably in mitigating harmonics around the switching frequency. This performance outperforms that of models utilizing LCL filters.

ACKNOWLEDGEMENTS

Author acknowledges the support of time and facilities from Ho Chi Minh University of Technology (HCMUT), VNU-HCM for this study.




REFERENCES

- [1] R. Mathew and P. P. K. Panikkar, "Inertial issues in renewable energy integrated systems and virtual inertia techniques," *International Journal of Power Electronics and Drive Systems (IJPEDS)*, vol. 15, no. 1, pp. 466–479, Mar. 2024, doi: 10.11591/ijpeds.v15.i1.pp466-479.
- [2] R. F. Edan, A. J. Mahdi, and T. M. A. Wahab, "Optimized proportional-integral controller for a photovoltaic-virtual synchronous generator system," *International Journal of Power Electronics and Drive Systems (IJPEDS)*, vol. 13, no. 1, pp. 509–519, Mar. 2022, doi: 10.11591/ijpeds.v13.i1.pp509-519.
- [3] M. Chen, D. Zhou, and F. Blaabjerg, "Modelling, implementation, and assessment of virtual synchronous generator in power systems," *Journal of Modern Power Systems and Clean Energy*, vol. 8, no. 3, pp. 399–411, 2020, doi: 10.35833/MPCE.2019.000592.
- [4] G. Ala *et al.*, "Virtual synchronous generator: an application to microgrid stability," in *2022 11th International Conference on Renewable Energy Research and Application (ICRERA)*, IEEE, Sep. 2022, pp. 151–157. doi: 10.1109/ICRERA55966.2022.9922782.
- [5] J. W. Shim, G. Verbic, and K. Hur, "Stochastic eigen-analysis of electric power system with high renewable penetration: impact of changing inertia on oscillatory modes," *IEEE Transactions on Power Systems*, vol. 35, no. 6, pp. 4655–4665, Nov. 2020, doi: 10.1109/TPWRS.2020.3000577.




- [6] D. Sharma, F. Sadeque, and B. Mirafzal, "Synchronization of inverters in grid forming mode," *IEEE Access*, vol. 10, pp. 41341–41351, 2022, doi: 10.1109/ACCESS.2022.3167521.
- [7] M. R. Amin and S. A. Zulkifli, "Modelling of virtual synchronous converter for grid-inverter synchronization in microgrids applications," *International Journal of Power Electronics and Drive Systems (IJPEDS)*, vol. 7, no. 4, pp. 1377–1385, Dec. 2016, doi: 10.11591/ijpeds.v7.i4.pp1377-1385.
- [8] H.-P. Beck and R. Hesse, "Virtual synchronous machine," in *2007 9th International Conference on Electrical Power Quality and Utilisation*, IEEE, Oct. 2007, pp. 1–6. doi: 10.1109/EPQU.2007.4424220.
- [9] J. Are Suul and S. D'Arco, "Comparative analysis of small-signal dynamics in virtual synchronous machines and frequency-derivative-based inertia emulation," in *2018 IEEE 18th International Power Electronics and Motion Control Conference (PEMC)*, IEEE, Aug. 2018, pp. 344–351. doi: 10.1109/EPEPMC.2018.8522010.
- [10] Z. Shi, J. Ruan, Y. Hong, M. Li, and D. Liu, "Dual-module VSG control strategy under unbalanced voltage conditions," *Journal of Power Electronics*, vol. 23, no. 6, pp. 923–934, Jun. 2023, doi: 10.1007/s43236-022-00587-8.
- [11] G. Li, F. Ma, C. Wu, M. Li, J. M. Guerrero, and M.-C. Wong, "A generalized harmonic compensation control strategy for mitigating subsynchronous oscillation in synchronverter based wind farm connected to series compensated transmission line," *IEEE Transactions on Power Systems*, vol. 38, no. 3, pp. 2610–2620, May 2023, doi: 10.1109/TPWRS.2022.3191061.
- [12] Z. Kustanovich, S. Shrivatri, H. Yin, F. Reissner, and G. Weiss, "Synchronverters with fast current loops," *IEEE Transactions on Industrial Electronics*, vol. 70, no. 11, pp. 11357–11367, Nov. 2023, doi: 10.1109/TIE.2022.3229275.
- [13] Q.-C. Zhong and G. Weiss, "Synchronverters: inverters that mimic synchronous generators," *IEEE Transactions on Industrial Electronics*, vol. 58, no. 4, pp. 1259–1267, Apr. 2011, doi: 10.1109/TIE.2010.2048839.
- [14] W. Schulze, P. Weber, M. Suriyah, and T. Leibfried, "Grid-forming synchronverter-based control method with current limiting method for grid-side converters of converter-based generation plants," in *21st Wind & Solar Integration Workshop (WIW 2022)*, Institution of Engineering and Technology, 2022, pp. 394–401. doi: 10.1049/icp.2022.2802.
- [15] S. Dong and Y. C. Chen, "A method to directly compute synchronverter parameters for desired dynamic response," *IEEE Transactions on Energy Conversion*, vol. 33, no. 2, pp. 814–825, Jun. 2018, doi: 10.1109/TEC.2017.2771401.
- [16] A. Rodriguez-Cabero, J. Roldan-Perez, and M. Prodanovic, "Synchronverter small-signal modelling and eigenvalue analysis for battery systems integration," in *2017 IEEE 6th International Conference on Renewable Energy Research and Applications (ICRERA)*, IEEE, Nov. 2017, pp. 780–784. doi: 10.1109/ICRERA.2017.8191165.
- [17] K. Y. Yap, C. M. Beh, and C. R. Sarimuthu, "Fuzzy logic controller-based synchronverter in grid-connected solar power system with adaptive damping factor," *Chinese Journal of Electrical Engineering*, vol. 7, no. 2, pp. 37–49, Jun. 2021, doi: 10.23919/CJEE.2021.000014.
- [18] R. Rosso, J. Cassoli, G. Buticchi, S. Engelken, and M. Liserre, "Robust stability analysis of LCL filter based synchronverter under different grid conditions," *IEEE Transactions on Power Electronics*, vol. 34, no. 6, pp. 5842–5853, Jun. 2019, doi: 10.1109/TPEL.2018.2867040.
- [19] S. S. Pore. and P. R. Jadhav., "Filters for grid connected self-synchronized synchronverter," in *2019 4th International Conference on Recent Trends on Electronics, Information, Communication & Technology (RTEICT)*, IEEE, May 2019, pp. 551–555. doi: 10.1109/RTEICT46194.2019.9016821.
- [20] R. Rosso, J. Cassoli, S. Engelken, G. Buticchi, and M. Liserre, "Analysis and design of LCL filter based synchronverter," in *2017 IEEE Energy Conversion Congress and Exposition (ECCE)*, IEEE, Oct. 2017, pp. 5587–5594. doi: 10.1109/ECCE.2017.8096930.
- [21] D. Li, Q. Zhu, S. Lin, and X. Y. Bian, "A self-adaptive inertia and damping combination control of VSG to support frequency stability," *IEEE Transactions on Energy Conversion*, vol. 32, no. 1, pp. 397–398, Mar. 2017, doi: 10.1109/TEC.2016.2623982.
- [22] F. Wang, L. Zhang, X. Feng, and H. Guo, "An adaptive control strategy for virtual synchronous generator," *IEEE Transactions on Industry Applications*, vol. 54, no. 5, pp. 5124–5133, Sep. 2018, doi: 10.1109/TIA.2018.2859384.
- [23] Q.-C. Zhong, P.-L. Nguyen, Z. Ma, and W. Sheng, "Self-synchronized synchronverters: inverters without a dedicated synchronization unit," *IEEE Transactions on Power Electronics*, vol. 29, no. 2, pp. 617–630, Feb. 2014, doi: 10.1109/TPEL.2013.2258684.
- [24] S. Dong and Y. C. Chen, "Adjusting synchronverter dynamic response speed via damping correction loop," *IEEE Transactions on Energy Conversion*, vol. 32, no. 2, pp. 608–619, Jun. 2017, doi: 10.1109/TEC.2016.2645450.
- [25] S. Dong and Y. C. Chen, "Improving active-power transfer capacity of virtual synchronous generator in weak grid," in *2019 20th Workshop on Control and Modeling for Power Electronics (COMPEL)*, IEEE, Jun. 2019, pp. 1–7. doi: 10.1109/COMPEL.2019.8769713.
- [26] M. Huang, F. Blaabjerg, Y. Yang, and W. Wu, "Step by step design of a high order power filter for three-phase three-wire grid-connected inverter in renewable energy system," in *2013 4th IEEE International Symposium on Power Electronics for Distributed Generation Systems (PEDG)*, IEEE, Jul. 2013, pp. 1–8. doi: 10.1109/PEDG.2013.6785603.
- [27] G. Feng, "A survey on analysis and design of model-based fuzzy control systems," *IEEE Transactions on Fuzzy Systems*, vol. 14, no. 5, pp. 676–697, Oct. 2006, doi: 10.1109/TFUZZ.2006.883415.
- [28] V. Thomas, K. S., and S. Ashok, "Fuzzy controller-based self-adaptive virtual synchronous machine for microgrid application," *IEEE Transactions on Energy Conversion*, vol. 36, no. 3, pp. 2427–2437, Sep. 2021, doi: 10.1109/TEC.2021.3057487.

BIOGRAPHIES OF AUTHORS






Tan Thien Tran    is an electrical engineer at Load Dispatch Department, Southern Regional National Load Dispatch Centre, Ho Chi Minh City, Vietnam. He received his B.Eng. degree in Electrical Engineering from Ho Chi Minh City University of Technology (HCMUT), VNU-HCM, in 2018. He was with Ho Chi Minh City Power Corporation – Electrical Testing Company as a High Voltage testing engineer from 2018 to 2020, then was with Cao Thang Technical College as a lecturer from 2020 to 2023. His research interests include the field of optimization and stability of power systems, renewable energy, power electronics, and its application in power system. He can be contacted at email: thientt.a2@nldc.evn.vn.






Quoc Dung Phan    was born in Saigon (now Ho Chi Minh City), Vietnam, in 1967. He received his Dipl.-Eng. degree in Electromechanical Engineering from Donetsk Polytechnic Institute, Donetsk City, USSR (now Ukraine), in 1991. He received his Ph.D. degree in Engineering Sciences from Kyiv Polytechnic Institute, Kyiv City, Ukraine, in 1995. Currently, he is an associate professor in the Faculty of Electrical and Electronics Engineering at Ho Chi Minh City University of Technology (HCMUT), Vietnam National University-Ho Chi Minh City (VNU-HCM), Vietnam. His research interests include power electronics (especially multilevel and multiphase converter topology and control), control of electric machines, wind and solar power systems, artificial intelligence, and smart grid. He can be contacted at email: pqdung@hcmut.edu.vn.



Bao Anh Nguyen    was born in Ho Chi Minh City, Vietnam, in 1985. He received the bachelor of engineering in Electrical Engineering from Ho Chi Minh City University of Technology (HCMUT), Vietnam National University - Ho Chi Minh City (VNU-HCM), in 2008. He received the master of engineering in Electrical Engineering from HCMUT, VNU-HCM, in 2011. At present, he is a researcher in the Faculty of Electrical and Electronics Engineering at HCMUT, VNU-HCM, Vietnam. His research interests include power electronics and control of electric machines. He can be contacted at email: ngbaoanh@hcmut.edu.vn.



Weng Kean Yew    was born in Selangor, Malaysia. He received the Ph.D. degree in Electrical Engineering from the National Energy University, Malaysia, in 2019. He is currently an assistant professor at Heriot-Watt University Malaysia, Putrajaya, Malaysia. His research interests include hybrid green power systems, renewable energy, artificial intelligence, and smart grids. He can be contacted at email: w.yew@hw.ac.uk.